

A CENTER-AVERAGED TWO-FLUID MODEL FOR WALL-BOUNDED BUBBLY FLOWS

A.E. Larreteguy^{†‡}, D.A. Drew[†], and R.T. Lahey, Jr.[†]

† Center for Multiphase Research, Rensselaer Polytechnic Institute

Troy, NY 12180, USA

‡ Centro Atómico Bariloche e Instituto Balseiro, CNEA

Bariloche, 8400 RN, Argentina

e-mail: axel@cab.cnea.gov.ar

RESUMEN

La correcta predicción de la concentración de gas (o fracción de vacío) cerca de paredes sólidas es aún un tema no resuelto, en parte debido a que generalmente se pasa por alto el hecho de que estos perfiles dependen de dos factores muy distintos: a) las fuerzas que actúan sobre las burbujas, y, b) las restricciones geométricas impuestas por la forma de las burbujas. Proponemos aquí un modelo de dos fluidos que involucra un promediado que llamaremos central (esto es, con una función de peso deltiforme localizada en el centro de cada burbuja), y una reinterpretación y postprocesamiento de los resultados obtenidos. El promediado central se utiliza solo para obtener las ecuaciones promediadas de la fase dispersa (burbujas), mientras que la fase continua (líquido) se promedia como es usual en el modelo de dos fluidos tradicional, utilizando el así llamado indicador de fase. Los resultados obtenidos con este modelo son postprocesados para reintroducir la geometría de las burbujas, y así obtener valores que representan cantidades medibles experimentalmente. La idea clave aquí es introducir el efecto de los dos factores nombrados en dos pasos sucesivos, independientes. El nuevo modelo puede ser implementado fácilmente en códigos desarrollados en base al modelo de dos fluidos tradicional. Al final de este trabajo se presentan comparaciones con resultados experimentales obtenidos por otros autores [19], que muestran en forma evidente las ventajas del modelo propuesto.

ABSTRACT

The accurate prediction of void fraction profiles near solid walls using the two-fluid model is still an unresolved issue. These profiles result from the combination of two factors: a) forces acting on the bubbles, and, b) geometric constraints imposed by their shape. We propose herein a two-fluid model that involves a center-averaging procedure for the disperse phase, and a reinterpretation and postprocessing of the results obtained. The center-averaged approach averages the disperse phase (bubbles) based on a center indicator function, while using the standard phase indicator averaging for the continuous phase (liquid). The solution fields obtained are then postprocessed to introduce the geometry of the bubbles in order to recover the values that should be representative of measured fields. The key idea here is to separate the geometric aspect from the dynamic aspect of the problem into two independent, successive steps. The new model may be easily incorporated into existing two-fluid model codes. Results obtained with the new model showing agreement with experimental data [19] are also presented.

INTRODUCTION

Despite numerous improvements to the two-fluid model for evaluating multiphase flows, there are several problems that have not yet been adequately addressed. One of these problems is the prediction of flows near solid walls or other situations involving highly localized concentrations of particles. The difficulties found in modeling some of these situations, however, arise more from a misinterpretation of the results of the two-fluid model than from some inherent complexity in the situation at hand.

Consider, for example, the case of an upwardly moving flow of a liquid containing mono-dispersed spherical bubbles near a vertical flat plate. A sheet of bubbles is observed [19] to form near the wall, with a void fraction profile that looks like an inverted parabola. There is zero void fraction at the wall, and void peaking occurs at approximately one bubble radius from it. This profile is the result of the combination of two factors, namely: a) the forces acting on the bubbles and, b) the geometric constraints imposed by the bubble's shape. The expectation is that the two-fluid model should give a good approximation to the measured profile. To this end, the usual approach [1], [27], is to include wall forces in the two-fluid model, and adjust them to obtain agreement with the experimental results. The "standard" two-fluid model, however, uses a phase indicator function for averaging the dispersed phase, hence leading to a mathematical representation in which both factors (flow dynamics and bubble geometry) are inextricably intermixed, and cannot be modeled and solved for separately.

We propose herein an approach that involves a different averaging procedure for the disperse phase and a reinterpretation of the results that will hopefully lead to easier ways of predicting these type of flows. A center-averaged approach involves averaging the disperse phase based on the dispersed phase's center indicator function, while using the phase indicator averaging for the continuous phase (the idea of a center indicator function is not completely new, and variations of it may be found in the literature [30], [12], [22], [2], [3]). The solution fields obtained are then postprocessed to introduce the geometry of the particles in order to recover the values that should be representative of measured fields. The key idea here is to separate the geometric aspect from the dynamic aspect of the problem into two independent, successive steps.

TWO-FLUID MODELING OF DISPERSE FLOWS

We present here a short review of what we might call the "standard" two-fluid model for dispersed flows. The term dispersed denotes a multi-component flow in which one of the phases may be termed as *continuous* (in the sense that any two points belonging to this component may be connected by a continuous curve lying entirely inside it), and the other as *dispersed* (i.e.: composed by separate individual units). Examples of such flows are: solid particles in gas, liquid drops in gas, bubbles in liquid, etc. In the following we will use the term *particle* to denote the individual units (i.e.: solid particles, drops, or bubbles). In the following, unless otherwise stated, we assume that the particles are spherical.

Generic Conservation Equations

The conservation equations associated with the motion of ordinary materials can be put in the generic form ([9], §8.1)

$$\frac{\partial \rho \Psi}{\partial t} + \nabla \cdot \rho \Psi \mathbf{u} = \nabla \cdot \mathbf{J} + \rho \mathbf{f} , \quad (1)$$

where ρ is the density, \mathbf{u} is the phasic velocity, Ψ is the conserved quantity, \mathbf{J} is its flux, and \mathbf{f} if its source density. In multicomponent materials, the previous equations are only valid inside each component. In addition, at the interface between materials, the following *jump conditions* must be fulfilled:

$$[\rho \Psi(\mathbf{u} - \mathbf{u}_i) + \mathbf{J}] \cdot \mathbf{n} = m . \quad (2)$$

These generic equations may be specialized to obtain the mass and momentum conservation principles, by making the substitutions given in the following table

Principle	Ψ	\mathbf{J}	\mathbf{f}	m
Mass	1	0	0	0
Momentum	\mathbf{u}	\mathbf{T}	\mathbf{g}	\mathbf{m}

where \mathbf{T} , \mathbf{g} and \mathbf{m} are, respectively, the stress tensor, the body force, and the interfacial force.

The Phase Indicator Function

The *phase indicator*, or *characteristic*, function, X_k , is defined by:

$$X_k(\mathbf{x}, t) = \begin{cases} 1 & \text{if } \mathbf{x} \in k \text{ at time } t, \\ 0 & \text{otherwise.} \end{cases} \quad (3)$$

The following relation, called *topological equation*, also holds ([9], §9.1.3) for the phase indicator function:

$$\frac{\partial X_k}{\partial t} + \mathbf{u}_i \cdot \nabla X_k = 0, \quad (4)$$

where \mathbf{u}_i is the interfacial velocity.

Averaged Balance Equations

We obtain the averaged balance equations by taking the product of the generic conservation equation with X_k , then performing the averaging process. After some manipulations we obtain:

$$\frac{\partial \overline{X_k \rho \Psi}}{\partial t} + \nabla \cdot \overline{X_k \rho \Psi \mathbf{u}} - \nabla \cdot \overline{X_k \mathbf{J}} - \overline{X_k \rho \mathbf{f}} = \overline{\rho \Psi \left(\frac{\partial X_k}{\partial t} + \mathbf{u} \cdot \nabla X_k \right)} - \overline{\mathbf{J} \cdot \nabla X_k}. \quad (5)$$

where $\overline{(\cdot)}$ denotes the ensemble averaging operator. Using the topological equation, Eq.(4), we can reduce the right hand side of Eq.(5), to obtain:

$$\frac{\partial \overline{X_k \rho \Psi}}{\partial t} + \nabla \cdot \overline{X_k \rho \Psi \mathbf{u}} - \nabla \cdot \overline{X_k \mathbf{J}} - \overline{X_k \rho \mathbf{f}} = \overline{[\rho \Psi (\mathbf{u} - \mathbf{u}_i) - \mathbf{J}] \cdot \nabla X_k}. \quad (6)$$

Conservation of mass and momentum for phase k in the average sense is therefore expressed as ([9],§11.3)

$$\frac{\partial \alpha_k \rho_k}{\partial t} + \nabla \cdot \alpha_k \rho_k \mathbf{u}_k = \Gamma_k \quad (7)$$

and,

$$\frac{\partial \alpha_k \rho_k \mathbf{u}_k}{\partial t} + \nabla \cdot \alpha_k \rho_k \mathbf{u}_k \mathbf{u}_k = \Gamma_k \mathbf{u}_k^m + \nabla \cdot \alpha_k (\mathbf{T}_k + \mathbf{T}_k^{Re}) + \alpha_k \rho_k \mathbf{g} + \mathbf{M}_k, \quad (8)$$

where we have introduced the ensemble averaged variables:

$$\alpha_k = \overline{X_k}, \quad \rho_k = \overline{X_k \rho} / \alpha_k, \quad \mathbf{u}_k = \overline{X_k \rho \mathbf{u}} / \alpha_k \rho_k. \quad (9)$$

In addition, we have defined the mass source

$$\Gamma_k = \overline{\rho (\mathbf{u} - \mathbf{u}_i) \cdot \nabla X_k}, \quad (10)$$

the average interfacial velocity

$$\mathbf{u}_{ki}^m = \overline{\rho \mathbf{u} (\mathbf{u} - \mathbf{u}_i) \cdot \nabla X_k} / \Gamma_k , \quad (11)$$

the average stress tensor

$$\mathbf{T}_k = \overline{X_k \mathbf{T}} / \alpha_k , \quad (12)$$

the interfacial force

$$\mathbf{M}_k = -\overline{\mathbf{T} \cdot \nabla X_k} , \quad (13)$$

and the Reynolds stress tensor

$$\mathbf{T}_k^{Re} = -\overline{X_k \rho \mathbf{u}'_k \mathbf{u}'_k} / \alpha_k , \quad (14)$$

where

$$\mathbf{u}'_k = \mathbf{u} - \mathbf{u}_k . \quad (15)$$

The mass source and the interfacial force must obey the following mass and momentum jump conditions

$$\sum_k \Gamma_k = 0 , \quad (16)$$

and

$$\sum_k (\mathbf{M}_k + \mathbf{u}_{ki}^m \Gamma_k) = \mathbf{m} . \quad (17)$$

where \mathbf{u}_{ki}^m is the interfacial velocity associated with mass transfer, and the force \mathbf{m} contains surface tension effects and must be modeled for each particular case.

The Rate of Change of Mass and The Number Density Equation

For the type of flows we are considering, the mass source may be modeled as:

$$\Gamma_d = -\Gamma_c = N''' \frac{dm}{dt} \quad (18)$$

where we denote the change of mass of the particle as $\frac{dm}{dt}$, and introduce the local particle number density, N''' . This variable can be calculated using the following conservation equation:

$$\frac{\partial N'''}{\partial t} + \nabla \cdot N''' \mathbf{u}_d = 0 , \quad (19)$$

where we have assumed no particle coalescence or break-up, and we have *postulated* that the averaged dispersed-phase velocity may be used as the particle velocity.

Equation (19), along with the mass and momentum conservation equations, are all that we need to solve the problem, provided we have models for the stress tensor and for the mass, momentum, and number density sources.

CENTER-AVERAGED TWO-FLUID MODEL FOR DISPERSE FLOWS

The Center Indicator Function

The *center indicator function*, η , is defined by

$$\eta(\mathbf{x}, t) = \sum_{i=1}^N \delta(\mathbf{x} - \mathbf{z}_i(t)) \quad (20)$$

where N is the total number of particles inside the whole domain Ω , and $\mathbf{z}_i(t)$ is the position of the center of the i^{th} particle at time t . Integrating η over the whole domain gives the total number of particles in the domain at time t :

$$\int_{\Omega} \eta(\mathbf{x}, t) dv = \int_{\Omega} \sum_{i=1}^N \delta(\mathbf{x} - \mathbf{z}_i(t)) dv = \sum_{i=1}^N \int_{\Omega} \delta(\mathbf{x} - \mathbf{z}_i(t)) dv = N . \quad (21)$$

Note that there exists something equivalent to the topological equation for η . In fact, if we are moving with the center of the particle, then the total derivative of η should remain null, that is:

$$\frac{\partial \eta}{\partial t} + \mathbf{u}_p \cdot \nabla \eta = 0 , \quad (22)$$

where now $\mathbf{u}_p = \frac{d\mathbf{z}}{dt}$ is the velocity of the center of the particle.

Relation between X_d and η

We look for a connection between the phase indicator function, X_d , and the center indicator function, η . For spherical particles, the phase indicator function can be written as:

$$X_d(\mathbf{x}, t) = \sum_{i=1}^N H(a_i(t) - |\mathbf{x} - \mathbf{z}_i(t)|) , \quad (23)$$

where H is the Heaviside step function, and a_i and \mathbf{z}_i are, respectively, the radius and the position of the center of the i^{th} particle. We can rewrite Eq(23) as:

$$X_d(\mathbf{x}, t) = \sum_{i=1}^N H(\bar{a}(\mathbf{z}_i, t) - |\mathbf{x} - \mathbf{z}_i(t)|) + X'_p(\mathbf{x}, t) , \quad (24)$$

where we have split the instantaneous value of the particle radius into a mean value and a perturbation

$$a_i(t) = \bar{a}(\mathbf{z}_i, t) - a'_i(t) = \int_{\Omega} \delta(\mathbf{x} - \mathbf{z}_i) \bar{a}(\mathbf{x}, t) d\mathbf{x} + a'_i(t) , \quad (25)$$

and introduce the *characteristic perturbation function*:

$$X'_d(\mathbf{x}, t) = \sum_{i=1}^N [H(a_i(t) - |\mathbf{x} - \mathbf{z}_i(t)|) - H(\bar{a}(\mathbf{z}_i, t) - |\mathbf{x} - \mathbf{z}_i(t)|)] \quad (26)$$

This characteristic perturbation is a field than can have the discrete values -1, 0, or 1, depending on the relation between the actual radius $a_i(t)$ and the average radius $\bar{a}(\mathbf{z}_i, t)$.

Remark 1 If we were to assume that both radius, $a_i(t)$ and $\bar{a}(\mathbf{z}_i, t)$, are equal at all times, for all the particles in all the realizations, we would get $X'_d(\mathbf{x}, t) = 0; \forall (\mathbf{x}, t) \in [\Omega \times \mathbf{T}]$, which is the appropriate mathematical expression for what is known in the literature as a **monodisperse** model.

The variable $\bar{a}(\mathbf{x}, t)$ is in fact an averaged field, which is no longer related to a specific particle or realization. Making the assumption that this is a slowly varying field, in the sense that it is approximately constant inside a ball of radius $\bar{a}(\mathbf{x}, t)$, and noting that the Heaviside function already restricts the distance $|\mathbf{x} - \mathbf{z}_i(t)|$ to this range, we may approximate $\bar{a}(\mathbf{z}_i, t)$ by $\bar{a}(\mathbf{x}, t)$ and manipulate the left hand side of Eq.(23) to obtain:

$$\begin{aligned} \sum_{i=1}^N H(\bar{a}(\mathbf{z}_i, t) - |\mathbf{x} - \mathbf{z}_i(t)|) &= \sum_{i=1}^N H(\bar{a}(\mathbf{x}, t) - |\mathbf{x} - \mathbf{z}_i(t)|) + X''_d(\mathbf{x}, t) \\ &= \sum_{i=1}^N \int_{\bar{\Omega}(\mathbf{x}, t)} \delta(\boldsymbol{\xi} - \mathbf{z}_i(t)) d\boldsymbol{\xi} + X''_d(\mathbf{x}, t) \\ &= \int_{\bar{\Omega}(\mathbf{x}, t)} \sum_{i=1}^N \delta(\boldsymbol{\xi} - \mathbf{z}_i(t)) d\boldsymbol{\xi} + X''_d(\mathbf{x}, t) = \int_{\bar{\Omega}(\mathbf{x}, t)} \eta dv + X''_d(\mathbf{x}, t) , \end{aligned} \quad (27)$$

where we define the domain

$$\bar{\Omega}(\mathbf{x}, t) = \{ \boldsymbol{\xi} \mid |\boldsymbol{\xi} - \mathbf{x}| \leq \bar{a}(\mathbf{x}, t) \} , \quad (28)$$

and have introduced the *characteristic error function*:

$$X''_d(\mathbf{x}, t) = \sum_{i=1}^N H(\bar{a}(\mathbf{z}_i, t) - |\mathbf{x} - \mathbf{z}_i(t)|) - \sum_{i=1}^N H(\bar{a}(\mathbf{x}, t) - |\mathbf{x} - \mathbf{z}_i(t)|) . \quad (29)$$

We define the volume averaging operator

$$\bar{f}^V(\mathbf{x}, t) = \frac{1}{v} \int_{\bar{\Omega}(\mathbf{x}, t)} f(\boldsymbol{\xi}, t) d\boldsymbol{\xi} , \quad (30)$$

where f is any function, and introduce the mean volume,

$$\bar{v}(\mathbf{x}, t) = |\bar{\Omega}(\mathbf{x}, t)| = \frac{4\pi\bar{a}^3}{3} . \quad (31)$$

We may then rewrite Eq.(23) using Eq.(27) to obtain:

$$X_d(\mathbf{x}, t) = \bar{v} \bar{\eta}^V + X'_d(\mathbf{x}, t) + X''_d(\mathbf{x}, t) . \quad (32)$$

The η -averaged Balance Equations for the Dispersed Phase

The process of ensemble-averaging performed in the previous section may be repeated almost exactly here, the only difference being the use of the center indicator function η instead of the phase indicator function X_d when averaging the generic balance equations. We denote this process as η -averaging.

We obtain the η -averaged balance equations by taking the product of the generic conservation equation with $\bar{v}\eta$, then performing the averaging process. We have, after some manipulation:

$$\frac{\partial \bar{v}\eta\rho\Psi}{\partial t} + \nabla \cdot \bar{v}\eta\rho\Psi\mathbf{u} - \bar{v}\eta\nabla \cdot \bar{\mathbf{J}} - \bar{v}\eta\rho\mathbf{f} = \overline{\rho\Psi \left(\frac{\partial \bar{v}\eta}{\partial t} + \mathbf{u} \cdot \nabla \bar{v}\eta \right)} , \quad (33)$$

where this time we chose not to split the term involving $\nabla \cdot \mathbf{J}$ into two terms as we did in the standard model. The conservation of mass and momentum equations for the dispersed phase in the η -average sense are expressed as:

$$\frac{\partial \bar{v} N^{\eta'''}}{\partial t} + \nabla \cdot \bar{v} N^{\eta'''} \rho_d^\eta \mathbf{u}_d^\eta = \Gamma_d^\eta , \quad (34)$$

and

$$\frac{\partial \bar{v} N^{\eta'''}}{\partial t} + \nabla \cdot \bar{v} N^{\eta'''} \rho_d^\eta \mathbf{u}_d^\eta = \nabla \cdot \bar{v} N^{\eta'''} \mathbf{T}_d^{\eta Re} + \bar{v} N^{\eta'''} \rho_d^\eta \mathbf{g} + \mathbf{I}_d^\eta + \Gamma_d^\eta \tilde{\mathbf{u}}_d^\eta . \quad (35)$$

where we have introduced the η -averaged bubble number density,

$$N^{\eta'''} = \bar{\eta} , \quad (36)$$

the η -averaged dispersed-phase density,

$$\rho_d^\eta = \frac{\bar{\eta} \rho}{N^{\eta'''}} , \quad (37)$$

the η -averaged dispersed-phase velocity,

$$\mathbf{u}_d^\eta = \frac{\bar{\eta} \rho \mathbf{u}}{\rho_d^\eta N^{\eta'''}} , \quad (38)$$

the η -averaged rate of mass change,

$$\Gamma_d^\eta = \overline{\rho \left(\frac{\partial \bar{v} \eta}{\partial t} + \mathbf{u} \cdot \nabla \bar{v} \eta \right)} , \quad (39)$$

the momentum-averaged dispersed-phase velocity,

$$\tilde{\mathbf{u}}_d^\eta = \overline{\rho \mathbf{u} \left(\frac{\partial \bar{v} \eta}{\partial t} + \mathbf{u} \cdot \nabla \bar{v} \eta \right)} / \Gamma_d^\eta , \quad (40)$$

the η -averaged *internal* force,

$$\mathbf{I}_d^\eta = \overline{\bar{v} \eta \nabla \cdot \mathbf{T}} , \quad (41)$$

and, the η -version of the Reynolds stress for the dispersed phase,

$$\mathbf{T}_d^{\eta Re} = - \frac{\overline{\eta \rho \mathbf{u}_d^{\eta'} \mathbf{u}_d^{\eta'}}}{N^{\eta'''}} , \quad (42)$$

where

$$\mathbf{u}_d^{\eta'} = \mathbf{u} - \mathbf{u}_d^\eta . \quad (43)$$

The η -averaged Rate of Change of Mass and Number Density Equation

The η -averaged rate of change of mass may be rewritten as:

$$\begin{aligned}\Gamma_d^\eta &= \overline{\rho \left(\frac{\partial \bar{v} \eta}{\partial t} + \mathbf{u} \cdot \nabla \bar{v} \eta \right)} = \frac{\partial \bar{v} N^{\eta'''}}{\partial t} + \nabla \cdot \bar{v} N^{\eta'''} \rho_d^\eta \mathbf{u}_d^\eta \\ &= N^{\eta'''} \left(\frac{\partial \bar{v} \rho_d^\eta}{\partial t} + \mathbf{u}_d^\eta \cdot \nabla \bar{v} \rho_d^\eta \right) + \bar{v} \rho_d^\eta \left(\frac{\partial N^{\eta'''}}{\partial t} + \nabla \cdot N^{\eta'''} \mathbf{u}_d^\eta \right) = N^{\eta'''} \frac{dm^\eta}{dt},\end{aligned}\quad (44)$$

where we introduce the rate of mass change of the average particle due to phase change,

$$\frac{dm^\eta}{dt} = \frac{\partial \rho_d^\eta \bar{v}}{\partial t} + \mathbf{u}_d^\eta \cdot \nabla \rho_d^\eta \bar{v},$$

and where, as in the standard two-fluid model, we *postulate* the use of the η -averaged dispersed-phase velocity as the carrying velocity of the conservation equation for the number density, which in the absence of particle coalescence and break-up is:

$$\frac{\partial N^{\eta'''}}{\partial t} + \nabla \cdot N^{\eta'''} \mathbf{u}_d^\eta = 0. \quad (45)$$

The η -averaged “Void Fraction”

We introduce an η -averaged “void fraction” as:

$$\alpha_d^\eta(\mathbf{x}, t) = \bar{v} N^{\eta'''}. \quad (46)$$

Remark 2 It is very important to note that, although Eq.(46) resembles the usual definition of void fraction, this is not so due to the fact that the meaning and values of $N^{\eta''''}$ and N''' are different. In the standard two-fluid model, the primitive variable is α_d , and the “number density” N''' is derived from it by dividing the void fraction by some suitably defined bubble volume. Consequently, N''' is defined in every point of the domain, even close to the walls. In our model, however, $N^{\eta'''}$ is the primitive variable, and α_d^η is derived from it. As $N^{\eta'''}$ is **not** defined for points in the domain closer than one bubble radius to the wall, then α_d^η is also **not** defined in that region, and should not be taken as representative of any measured field close to the walls.

We may rewrite the conservation equations in terms of the η -averaged void fraction α_d^η , to obtain:

$$\frac{\partial \alpha_d^\eta \rho_d^\eta}{\partial t} + \nabla \cdot \alpha_d^\eta \rho_d^\eta \mathbf{u}_d^\eta = \Gamma_d^\eta, \quad (47)$$

and

$$\frac{\partial \alpha_d^\eta \rho_d^\eta \mathbf{u}_d^\eta}{\partial t} + \nabla \cdot \alpha_d^\eta \rho_d^\eta \mathbf{u}_d^\eta \mathbf{u}_d^\eta = \nabla \cdot \alpha_d^\eta \mathbf{T}_d^{\eta Re} + \alpha_d^\eta \rho_d^\eta \mathbf{g} + \mathbf{I}_d^\eta + \Gamma_d^\eta \tilde{\mathbf{u}}_d^\eta. \quad (48)$$

A resemblance to the corresponding balance equation of the standard two-fluid model is now apparent. Note, however, that the divergence of the stress tensor does not appear explicitly in the momentum equation, for it is already included in the internal force term, \mathbf{I}_d^η .

Relationship between the Averaged Variables

We seek here for a way of recovering the standard values of the main variables from the η -averaged ones. In the following, the symbol \simeq indicates that an assumption has been made to obtain the corresponding relation. We will assume that all variables *except* N''' , α_d^η and \mathbf{u}_d^η , vary smoothly in regions of the size of the mean particle.

Remark 3 Following other authors, we call this assumption the small particle hypothesis. Note however, that this hypothesis is usually applied to all variables, including the number density, the void fraction, and the gas velocities. The key difference in our derivation is that we **do not** do that.

To find a relation between the standard and the modified void fractions, we apply the ensemble average operator to Eq.(32) , to obtain:

$$\begin{aligned}\alpha_d &= \overline{X_d} = \overline{\bar{v}\eta^V} + \overline{X'_d} + \overline{X''_d} = \overline{v}\overline{\eta^V} + \overline{X'_d} + \overline{X''_d} = \overline{v}\overline{\eta}^V + \overline{X'_d} + \overline{X''_d} \\ &= \overline{v}\overline{N^{\eta'''}}^V + \overline{X'_d} + \overline{X''_d} = \overline{v}\overline{N^{\eta'''}}^V + \overline{X'_d} + \overline{X''_d} = \overline{\alpha_d^\eta}^V + \overline{X'_d} + \overline{X''_d} .\end{aligned}\quad (49)$$

We must recall at this point that we have been using the mean radius $\bar{a}(\mathbf{x}, t)$ without really defining it. We do so now, by choosing the mean radius $\bar{a}(\mathbf{x}, t)$ (and therefore the mean volume $\bar{v}(\mathbf{x}, t)$) that gives us

$$\overline{X'_d} = 0 . \quad (50)$$

Under the small particle hypothesis we may assume:

$$\overline{X''_d} \simeq 0 . \quad (51)$$

Consequently, we may write,

$$\alpha_d = \overline{\alpha_d^\eta}^V . \quad (52)$$

Then, the standard void fraction, $\alpha_d(\mathbf{x}, t)$, is, *by definition*, the volume average of the η -averaged void fraction α_d^η in the region occupied by a mean particle centered at \mathbf{x} at time t .

Remark 4 Because of this relation, these void fractions differ considerably in regions where $N^{\eta'''}$ is not a smooth function (i.e., near walls). It is in these regions where α_d^η should not be taken as representative of any measured field, but as a dimensionless version of $N^{\eta'''}$. In the rest of the domain, however, both void fractions are almost indistinguishable.

Seeking a connection between \mathbf{u}_d and \mathbf{u}_d^η we may write

$$\overline{\alpha_d^\eta \rho_d^\eta \mathbf{u}_d^\eta}^V = \overline{\bar{v} N^{\eta'''}}^V \overline{\rho_d^\eta \mathbf{u}_d^\eta}^V = \overline{\overline{\bar{v} \eta \rho \mathbf{u}}}^V = \overline{\overline{\bar{v} \eta \rho \mathbf{u}}}^V \simeq \overline{\overline{\bar{v} \eta}^V \rho \mathbf{u}} = \overline{X_d \rho \mathbf{u}} = \alpha_d \rho_d \mathbf{u}_d , \quad (53)$$

where we use the assumptions of *monodispersion* and *no internal movement* inside the particle. Then, we recover the standard dispersed-phase velocity applying the volume averaging operator

$$\mathbf{u}_g = \overline{\alpha_d^\eta \rho_d^\eta \mathbf{u}_d^\eta}^V / \alpha_d \rho_d . \quad (54)$$

Using the small particle hypothesis, the averaged densities may simply be considered to be approximately equal, that is,

$$\rho_d^\eta \simeq \rho_d . \quad (55)$$

A COMPLETE MODEL FOR BUBBLY FLOWS

A *bubbly flow* is a disperse flow of small gas bubbles in a liquid. One of the main features of this type of flow is the big difference in densities of both phases, that is $\rho_g \ll \rho_l$, where we replaced the subindices d by

g , and c by l , to stress the fact that this is only valid for bubbly flow. In the following, we make suitable approximations and write a complete model for this type of flow.

Relation between Internal and Interfacial Forces

Neglecting all movements inside the bubble but those due to slow expansions or compressions, the total contribution of the internal forces, \mathbf{I}_g^η , may be easily related to the interfacial forces. In this case, $\nabla \cdot \mathbf{T}$ is spatially constant inside the bubble, so

$$\int_{\Omega_b} \nabla \cdot \mathbf{T} dv = v \nabla \cdot \mathbf{T} , \quad (56)$$

where v is the bubble volume and Ω_b is the space occupied by the bubble. Using the divergence theorem we write

$$\int_{\Omega_b} \nabla \cdot \mathbf{T} dv = \int_{\partial\Omega_b} \mathbf{T}_{gi} \cdot \mathbf{n}_{gi} dA = \int_{\partial\Omega_b} (\mathbf{T}_{li} + \frac{\sigma}{2r_b} \mathbf{I}) \cdot \mathbf{n}_{gi} dA = - \int_{\partial\Omega_b} \mathbf{T}_{li} \cdot \mathbf{n}_{li} dA . \quad (57)$$

where the subindex ki indicates interface (phase k side) and $\partial\Omega_b$ indicates the surface of the bubble. Then, combining the last two equations we obtain

$$\nabla \cdot \mathbf{T} = - \frac{\int_{\partial\Omega_b} \mathbf{T}_{li} \cdot \mathbf{n}_{li} dA}{v} , \quad (58)$$

and the total internal force can then be expressed as

$$\mathbf{I}_g^\eta = - \bar{v} \frac{\eta}{v} \overline{\int_{\partial\Omega_b} \mathbf{T}_{li} \cdot \mathbf{n}_{li} dA} . \quad (59)$$

In this way, the resultant of the internal force has been related to the resultant of the forces applied by the liquid to the surface of the bubble.

Model for the Interfacial Force

The force \mathbf{I}_g^η , which we are now going to call the *interfacial force*, is split into two forces, one dependent on the mean field values, and the other on the fluctuations around these values. We define the fluctuating force as

$$\begin{aligned} \mathbf{I}'_g &= - \bar{v}\eta \frac{1}{v} \overline{\int_{\partial\Omega_b} \mathbf{T}_{li} \cdot \mathbf{n}_{li} dA} + \bar{v}\eta \frac{1}{v} \overline{\int_{\partial\Omega_b} \mathbf{T}_{li} \cdot \mathbf{n}_{li} dA} \\ &= - \bar{v}\eta \frac{1}{v} \overline{\int_{\partial\Omega_b} \mathbf{T}_{li} \cdot \mathbf{n}_{li} dA} + \alpha_g^\eta \frac{1}{v} \overline{\int_{\partial\Omega_b} \mathbf{T}_{li} \cdot \mathbf{n}_{li} dA} = \mathbf{I}_g^\eta - \bar{\mathbf{I}}_g , \end{aligned} \quad (60)$$

where we introduce the mean interfacial force

$$\bar{\mathbf{I}}_g = \alpha_g^\eta \frac{1}{v} \overline{\int_{\partial\Omega_b} \mathbf{T}_{li} \cdot \mathbf{n}_{li} dA} . \quad (61)$$

The mean force will be modeled taking into account only the mean pressure forces on the mean bubble, and neglecting viscous stresses. We have:

$$\bar{\mathbf{I}}_g \simeq \alpha_g^\eta \nabla p_l . \quad (62)$$

The fluctuating force is modeled in the usual way. The only difference is the use of the η -averaged variables for the dispersed phase quantities. The force \mathbf{I}'_g is expanded as

$$\mathbf{I}'_g = \mathbf{I}^{VM} + \mathbf{I}^L + \mathbf{I}^D + \mathbf{I}^{TD} \quad (63)$$

where the four forces are, respectively, those due to virtual mass, lift, drag, and turbulent dispersion. The virtual mass accounts for the effect of acceleration of the liquid displaced by the bubbles, and can be modeled as[7]

$$\mathbf{I}^{VM} = \alpha_g^\eta \rho_l C_{VM} \left[\left(\frac{\partial \mathbf{u}_l}{\partial t} + \mathbf{u}_l \cdot \nabla \mathbf{u}_l \right) - \left(\frac{\partial \mathbf{u}_g^\eta}{\partial t} + \mathbf{u}_g^\eta \cdot \nabla \mathbf{u}_g^\eta \right) \right] , \quad (64)$$

where the virtual mass coefficient C_{VM} is 0.5 for dilute potential flow.

The lift force is calculated from potential flow theory, and can be expressed as [8]:

$$\mathbf{I}^L = \alpha_g^\eta \rho_l C_L \mathbf{u}_r^\eta \times (\nabla \times \mathbf{u}_l) , \quad (65)$$

where we introduce the η -averaged relative velocity

$$\mathbf{u}_r^\eta = \mathbf{u}_l - \mathbf{u}_g^\eta . \quad (66)$$

The lift coefficient C_L has been found to be about 0.1 for fully developed vertical upflow of spherical particles in a pipe [28],[14], although different values have been found to be adequate in other types of flows [29], [7], [8], [27], [18].

The drag force may be expressed as

$$\mathbf{I}^D = \alpha_g^\eta \rho_l C_D \frac{3}{8} \frac{|\mathbf{u}_r^\eta|}{r_b} \mathbf{u}_r^\eta + \mathbf{D}_W , \quad (67)$$

where the drag coefficient C_D is defined after Tomiyama [27], with a void fraction correction based on that of Ishii [11] to include interaction between bubbles, that is:

$$C_D = \frac{1}{\alpha_l} \max \left[\frac{24}{Re_D} (1 + 0.15 Re_D^{0.687}) , \frac{8}{3} \frac{Eo}{Eo + 4} \right] , \quad (68)$$

which is valid for contaminated systems (i.e.: tap water). Here, Re_D is the bubble Reynolds number based on the bubble diameter, D_b , and the relative velocity, \mathbf{u}_r^η . The Eötvös number, Eo , defined by

$$Eo = \frac{g(\rho_l - \rho_g) D_b^2}{\sigma} , \quad (69)$$

represents the relative importance between buoyancy forces and surface tension, and has been included to take into account the increased drag observed in non-spherical bubbles. The additional term, \mathbf{D}_W , is a correction to the bulk drag due to the presence of solid walls. Following the model proposed by Lopez de Bertodano [17], based on the concept of bubbles sliding on the laminar sublayer, we define this *wall drag* as:

$$\mathbf{D}_W = - \alpha_g^\eta \rho_l C_{WD} \frac{3}{4} \frac{\nu_l}{r_b} \frac{\mathbf{u}_g^\eta}{(d_w - r_b)} , \quad (70)$$

where d_w is the distance from the center of the mean bubble to the nearest wall. In the present work, the coefficient C_{WD} is taken to be unity.

The last term, the turbulent dispersion force, is perhaps the most controversial of all of them since no widely accepted model exists to date. We use here the model proposed by Carrica et al. in [5]

$$\mathbf{I}^{TD} = - \alpha_g^\eta \rho_l C_{TD} C_D \frac{3}{8} \frac{|\mathbf{u}_r^\eta|}{r_b} \nu_t \frac{\nabla \alpha_g^\eta}{\alpha_g^\eta} , \quad (71)$$

where the turbulent dispersion coefficient C_{TD} is defined by

$$C_{TD} = Sc_b^{-1} = \frac{\nu_b}{\nu_t} , \quad (72)$$

where Sc_b is the bubble Schmidt number, which relates the turbulent difusivity ν_t of a passive scalar to the bubble diffusivity ν_b . Some evidence [16] shows that for the case of small solid particles the Schmidt number should be between 0.7 and 1.0; we have taken here the value 1.0. Finally, it is important to take into account in the turbulent dispersion force the effect of the additional turbulence ν_{bt} produced by the bubbles, which adds to the effective turbulent viscosity ν_t . In this work, we have chosen for this additional viscosity the model of Sato [25]:

$$\nu_{bt} = 1.2 \alpha_g^\eta r_b |\mathbf{u}_r^\eta| ,$$

which is strictly valid for $\alpha_g < 0.01$.

Remark 5 *These four forces were originally developed for the standard two-fluid model. Their use in the present two-fluid model is not, however, an “approximation”. We are really claiming here that, whether consciously or not, all the authors who have developed these force models over the years had in mind our present interpretation of the number density (i.e.: $N^{\eta''}$), although they put the resultant forces into the standard two-fluid model, which has really a different interpretation (i.e.: N''). The origin of many of the difficulties found when trying to predict void fraction profiles near walls may easily be traced back to these inconsistent interpretations of the number density.*

Momentum Equation for the Dispersed Phase

Taken into account the small density of the dispersed phase, and neglecting all movements inside the bubble except those due to slow expansion or compression, we may *neglect all terms except the internal forces*, and simply rewrite Eq.(48) as an internal self-balance, that is

$$\mathbf{I}_g^\eta = 0 . \quad (73)$$

Therefore, after dividing all terms by $\rho_l \alpha_g^\eta$, the momentum balance for the dispersed phase can be finally written as

$$\begin{aligned} & \frac{1}{\rho_l} \nabla p_l + C_{VM} \left[\left(\frac{\partial \mathbf{u}_l}{\partial t} + \mathbf{u}_l \cdot \nabla \mathbf{u}_l \right) - \left(\frac{\partial \mathbf{u}_g^\eta}{\partial t} + \mathbf{u}_g^\eta \cdot \nabla \mathbf{u}_g^\eta \right) \right] + C_L \mathbf{u}_r^\eta \times (\nabla \times \mathbf{u}_l) \\ & + C_D \frac{3}{8} \frac{|\mathbf{u}_r^\eta|}{r_b} \mathbf{u}_r^\eta - C_{WD} \frac{3}{4} \frac{\nu_l}{r_b} \frac{\mathbf{u}_g^\eta}{(d_w - r_b)} - C_{TD} C_D \frac{3}{8} \frac{|\mathbf{u}_r^\eta|}{r_b} \frac{\nu_t}{Sc_b} \frac{\nabla \alpha_g^\eta}{\alpha_g^\eta} = 0 \end{aligned} \quad (74)$$

Numerical Results

Let us now consider the case of an upward turbulent bubbly boundary layer along a vertical flat plate. Experimental results for this case have been obtained by Moursali, Marie and Bataille [19]. A sketch of the experiment is shown in Fig.1. Air bubbles are injected below the leading edge of the plate into a uniform flow of water with a free-stream velocity of $U_0 = 1.0m/s$. Although the experiment was carried out for three different inlet void fractions, we only consider here the results corresponding to the case $\alpha_0 = 0.01$, for it is the only case in which the radius of the bubbles may be considered uniform, with $r_b \simeq 1.5mm$. These bubbles were also observed to be slightly non-spherical. Four measuring stations were defined, at $x = 0.07, 0.2, 1.0$ and $1.5m$; however, only void fraction profiles for the third station are shown in [19].

In order to simulate this flow, the proposed model has been implemented in the multiphase code CFDShipM v2.1 [4], [15], [21], which was developed at Rensselaer Polytechnic Institute. This code is based on the single-phase code CFDShip-IOWA [23], [26], which was developed at the Iowa Institute of Hydraulics Research. The liquid solver is based on the Finite Analytic Coefficient method for the velocities, with a pressure correction equation for the pressure. The gas solver uses a TVD scheme [24] for the gas velocities and the bubble number density.

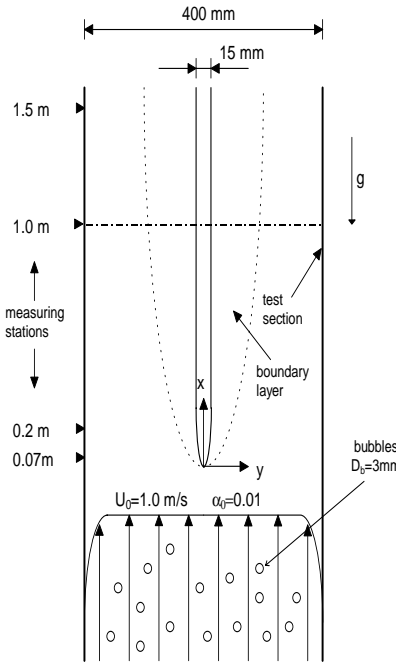


Figure 1: Sketch of the experiment

Since CFDShipM is a 3D code, a 3D grid of $108 \times 70 \times 3$ was used, for a total of 22680 nodes. Due to the symmetry of the case, only the right half of the domain was considered. A 2D cut of the grid and a magnification of the leading edge zone is shown in Fig. 2. A fine discretization at the wall is required to simulate the liquid boundary layer, but it is not needed for the gas problem.

In the present work, two-way coupling between gas and liquid solutions is not considered. Consequently, the liquid problem has been solved first, and its solution was used to evaluate the gas problem. The total CPU time for the whole problem was about 2 hours in a Cray T90.

The liquid problem may be considered standard. The results obtained with the $k - \epsilon$ model compare very well with the results available for turbulent boundary layers. Isolines of velocities, pressure and turbulent quantities are shown in Figs. 3 and 4

The isolines of η -averaged gas velocities are shown in Fig. 5. As expected, the vertical gas velocities are found to be greater than the corresponding liquid velocities due to the relative rise velocities of the bubbles. The horizontal gas velocities are high and positive near the leading edge region, due to the local pressure peak. Above this zone, however, the lift force prevails and the gas velocities have relatively small negative values, indicating that the bubbles are being slowly pushed towards the wall as they rise along the plate. As the bubbles approach the wall, the wall drag force slows them down until the lift force reverses sign, thus preventing the bubbles from getting closer to the wall.

The η -averaged and the postprocessed void fractions α_g^η and α_g are shown in Fig. 6. It should be noted that, in cases like this in which an almost δ -function like number density profile is found, the peak value of the η -averaged void fraction strongly depends on the grid spacing; the postprocessed void fraction, however,

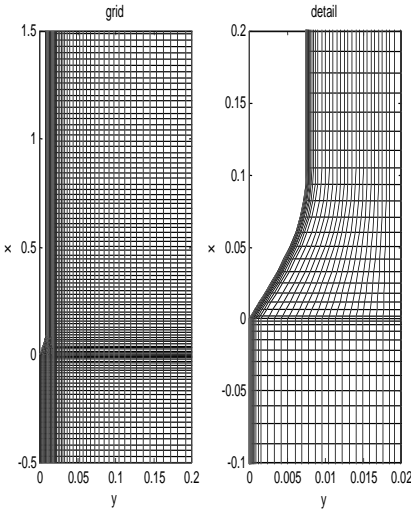


Figure 2: Domain discretization

does not.

Although the η -averaged gas velocities and void fractions are really not defined in the near-wall region (closer than one bubble radius) they have been arbitrarily set to zero in the calculations, for this makes it easy to compute the volume averaged values in the postprocessing step.

Note that the value of the postprocessed variables at any point takes into account the contribution of all bubbles that can touch that particular point, thus giving a good approximation to the values that would be measured using any kind of point-like probe.

The plots of liquid and gas velocities at the 3rd station (i.e.: $x=1.0\text{m}$) are shown in Figs. 7 and 8. Both the η -averaged and the postprocessed values are plotted for the gas velocities. Unfortunately, no gas velocity profiles are presented in [19], so comparison against measured velocities is not possible. Fig. 7 show that, far from the wall, both u_g^η and u_g have similar values, as expected, and the relative vertical velocity is constant and equal to the terminal rise velocity of the bubbles in a stagnant fluid. Close to the wall, however, the bubbles are slowed down due to the increased wall drag. The horizontal velocities plotted in Fig. 8 clearly show the effect of the lift on the bubbles, including the lift reversal that occurs close to the wall due to the action of the wall drag. In this case the η -averaged horizontal velocity is indeed a reasonably smooth function, and the difference between pre- and postprocessed velocities is quite small.

Both measured and calculated void fraction profiles are shown in Fig. 9. Excellent agreement between the results of Moursali, Marie and Bataille, and the postprocessed void fraction obtained with the code is evident. Our intention is not, however, to claim that we have found the ultimate model for bubble-wall interactions, but to show the similarity in the general shape of calculated and measured void fraction profiles obtained by applying our proposed model. We must always keep in mind that the value of the peak depends on the values chosen for the constants used to model the forces (i.e.: C_{VM}, C_L, C_{TD} and C_{WD}), let alone two-way coupling effects. The present results have been obtained with the following set of values: $C_{VM} = 0.5$, $C_L = 0.29$, $C_{TD} = 1.0$, $C_{WD} = 1.0$. The value of the lift coefficient C_L was obtained with the correlation proposed by Tomiyama [27].

In our calculations, we explored other values of the turbulent dispersion coefficient, ranging from 0 to 1.5, obtaining variations of up to 50% in the value of the void fraction peak. The results were also sensitive

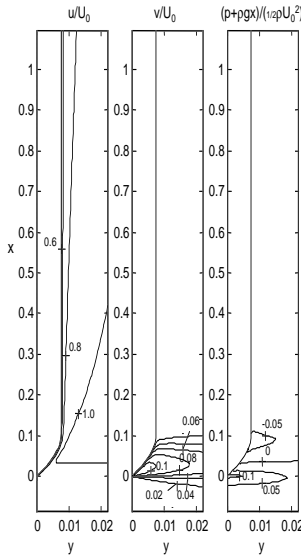


Figure 3: Isolines of liquid velocity and pressure

to the model used for the bubble induced turbulence, for it directly affects the turbulent dispersion forces by increasing the effective viscosity. The sensitivity to the other coefficients should also be explored in the future. Note, however, that only C_{WD} is directly related to the presence of solid walls, and thus it could be determined by comparison against careful measurements of gas velocity profiles near walls. The rest of the coefficients, which also await a careful determination, are relevant in the whole domain.

CONCLUSIONS

A center-averaged two-fluid model has been developed. The main difference from the standard two-fluid model is the use of a center-indicator function instead of the usual phase indicator function for averaging purposes, and a reinterpretation of the bubble number density.

The present model takes into account steep changes in bubble concentrations, allowing strongly non-linear variations of the number density in regions smaller than a bubble diameter. This results in a model capable of reproducing void fraction and velocity profiles near solid walls.

The dynamic and geometric factors contributing to the dispersed phase solution near solid walls have been successfully separated into two independent, successive steps. The first involves solving the problem for the newly defined center-averaged gas velocities and number densities, while the second is a purely geometric postprocessing step for recovering the values that are representative of measured quantities.

The model has been coded into an existing standard multiphase code. The modification required little effort, because it reduces to adding a postprocessing step, which in fact can be made off-line unless two-way coupling is required. The results obtained have been compared against experimental results obtained by other authors, showing that it is indeed a promising technique for solving wall bounded multiphase flows in situations in which the size of the bubbles make it unreasonable to take them as point particles.

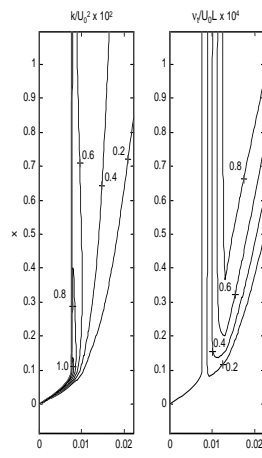


Figure 4: Isolines of turbulent kinetic energy and eddy viscosity

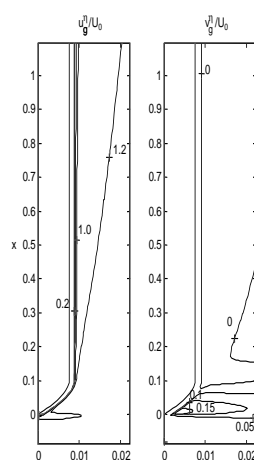


Figure 5: Isolines of center-averaged gas velocities

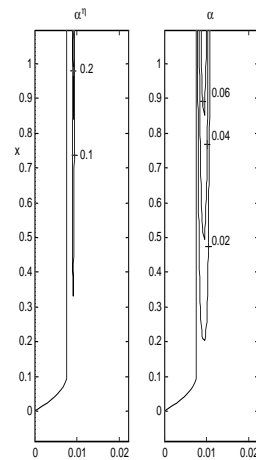


Figure 6: Isolines of center-averaged and postprocessed void fraction

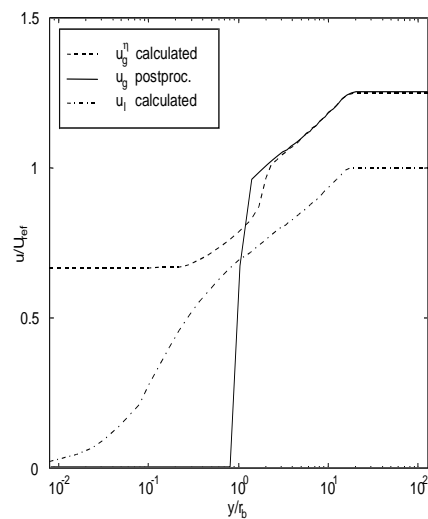


Figure 7: Cut of vertical velocities at $x=1.0\text{m}$

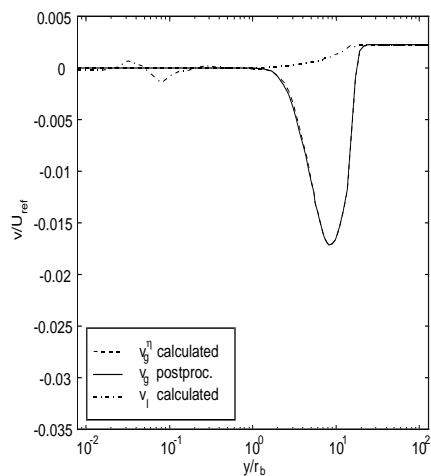


Figure 8: Cut of horizontal velocities at $x=1.0\text{m}$

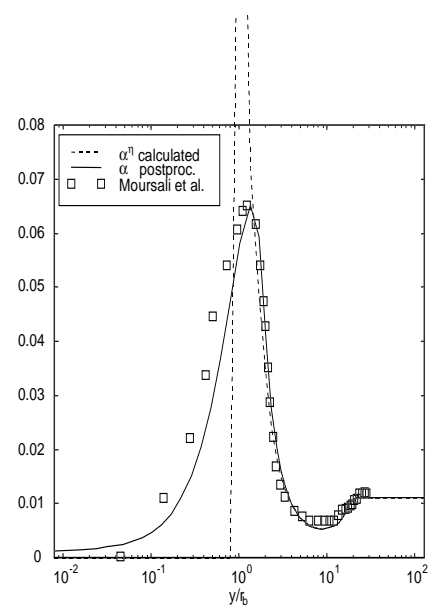


Figure 9: Cut of void fraction at $x=1.0\text{m}$

ACKNOWLEDGEMENTS

This work was sponsored by the Office of Naval Research under Grant N00014-96-1-0479, and was supported in part by a grant of HPC time from the DoD HPC centers ARL and ARSC.
The assistance of Fundación Antorchas (Argentina) in this project is also gratefully acknowledged.

References

- [1] Antal S.P., Lahey Jr. R.T., Flaherty J.E., *Analysis of Phase Distribution in Fully Developed Laminar Bubbly Two-Phase Flow*, Int. J. Multiphase Flow **17**, 635-652, 1991.
- [2] Biesheuvel A., Gorissen W.C.M., *Void Fraction Disturbances in a Uniform Bubbly Flow*, Int. J. Multiphase Flow, **16**, 211-231, 1990.
- [3] Biesheuvel A., Spoelstra S., *The Added Mass Coefficient of a Dispersion of Spherical Gas Bubbles in Liquid*, J. Fluid Mech. **148**, 301-318, 1989.
- [4] Carrica P. M., Bonetto F., Drew D.A., Lahey Jr. R.T. , *A Polydisperse Model for Bubbly Two-Phase Flow Around a Surface Ship*, accepted for publication in Int. J. Multiphase Flow, 1998.
- [5] Carrica P. M., Bonetto F., Drew D.A., Lahey Jr. R.T. , *The Interaction of Background Ocean Air Bubbles with a Surface Ship*, Int. J. Num. Meth. Fluids **28**, 571-600, 1998.
- [6] Drew D.A., Lahey R.T. Jr., *Aplication of General Constitutive Principles to the Derivation of Multi-dimensional Two-Phase Flow Equations*, Int. J. Multiphase Flow **5**, 243, 1979.
- [7] Drew D.A., Lahey R.T. Jr., *The Virtual Mass and Lift Force on a Sphere in Rotating and Straining Inviscid Flow*, Int. J. Multiphase Flow **13**, 113, 1987.
- [8] Drew D.A., Lahey R.T. Jr., *Some Supplemental Analysis on the Virtual Mass and Lift Force on a Sphere in Rotating and Straining Inviscid Flow*, Int. J. Multiphase Flow **16**, 1127, 1990.
- [9] Drew D.A., Passman S.L., *Theory of multicomponent fluids*, App. Math. Sci. **135**, Springer, 1998.
- [10] Ishii M., *Thermo-Fluid Dynamic Theory of Two-Phase Flow*, Eyrolles, Paris, 1975.
- [11] Ishii M., *Two-Fluid Model for Two-Phase Flow*, 2nd Int. Workshop on Two-Phase Flow Fundamentals, Rensselaer Polytechnic Institute, Troy, NY, 1987.
- [12] Koch D.L., *Kinetic Theory for a Monodisperse Gas-Solid Suspension*, Phys. Fluids A **2**, 1711-1723, 1990.
- [13] Lahey Jr. R.T., Drew D.A., *The Current State-of-the-Art in Modeling of Vapor/Liquid Two-Phase Flows*, ASME Paper 90-WA/HT-13, 1990.
- [14] Lahey Jr. R.T., Lopez de Bertodano M., Jones Jr. O.C., *Phase Distribution Phenomena in Complex Geometry Conduits*, Nuclear Eng. and Design **141**, 177-201, 1993.
- [15] Larreteguy A.E., Drew D.A., Carrica P.M., Bonetto F., *A Numerical Model for Three Dimensional Polydisperse Bubbly Flows around Surface Ships*, IV World Congress in Computational Mechanics, Buenos Aires, Argentina, July 1998. Published in Computational Mechanics: New Trends and Applications, E. Oñate, S. Idelsohn (Eds.), CIMNE, Barcelona, España, 1998.
- [16] Loth E., *Model of Two-Phase Turbulent Dispersion in a Planar Free Shear Layer*, AIAA Aerospace Sciences Meeting, Jan. 1997.

- [17] Lopez de Bertodano M., *Turbulent Bubbly Two-Phase Flow in a Triangular Duct*, Ph.D. Thesis, Rensselaer Polytechnic Institute, Troy, NY, USA, 1992.
- [18] Moraga F., *Lateral Forces on Rigid Spheres in Turbulent Uniform Shear Flow*, Ph.D. Thesis, Rensselaer Polytechnic Institute, Troy, NY, USA, 1998.
- [19] Moursali E., Marié J.L., Bataille J., *An Upward Turbulent Bubbly Boundary Layer along a Vertical Flat Plate*, Int. J. Multiphase Flow **21**, 107-117, 1995.
- [20] Park J.W., *Void Wave Propagation in Two-Phase Flow*, Ph.D. Thesis, Rensselaer Polytechnic Institute, Troy, NY, USA, 1992.
- [21] Paterson E., Hyman M., Stern F., Carrica P.M., Bonetto F., Drew D.A., Lahey R.T. Jr., *Near and Far-Field CFD for a Naval Combatant Including Thermal-Stratification and Two-Fluid Modeling*, proc. 21st Symp. on Naval Hydrodynamics, Trondheim, Norway, 1996.
- [22] Sangani A.S., Didwania A.K., *Dispersed Phase Stress Tensor in Flows of Bubble Liquids at Large Reynolds Numbers*, J. Fluid Mech. **248**, 27-54, 1993.
- [23] Stern F., Paterson E., Tahara Y., *CFDSHIP-IOWA: Computational Fluid Dynamics Method for Surface-Ship Boundary Layers and Wake and Wave Fields*, Iowa Institute of Hydraulic Research Report 666, Iowa City, USA, 1996.
- [24] Sweby P.K., *High Resolution TVD Schemes Using Flux Limiters*, in Large-Scale Computations in Fluid Mechanics, AMS, Providence, RI, USA, 1985.
- [25] Sato Y., Sadatomi M., Sekoguchi K., *Momentum and Heat Transfer in Two-Phase Bubble Flow-I*, Int. J. Multiphase Flow **7**, 167-177, 1981.
- [26] Tahara Y., Stern F., Rosen B., *An Interactive Approach for Calculating Ship Boundary Layers and Wakes for Nonzero Froude Number*, J. of Comp. Phys. **98**, p. 33, 1992.
- [27] Tomiyama A., *Struggle with Computational Bubble Dynamics*, Third Int. Conf. on Multiphase Flows, ICMF'98, Lyon, France, June 8-12, 1998.
- [28] Wang S.K., *Three-dimensional Turbulence Structure Measurements in Air/Water Two-Phase Flow*, Ph.D. Thesis, Rensselaer Polytechnic Institute, Troy, NY, 1986.
- [29] Wang S.K., Lee S.J., Jones O.C., Lahey R.T. Jr., *3D Turbulence Structure and Phase Distribution Measurements in Bubbly Two-Phase Flow*, Int. J. Multiphase Flow **13**, 327-343, 1987.
- [30] Zhang D.Z., Prosperetti A., *Averaged Equations for Inviscid Disperse Two-Phase Flow*, J. Fluid Mech. **267**, 185-219, 1994.